American Mineralogist, Volume 58, pages 765–770, 1973

Molecular Orbital Calculations on Beryllium and Boron Oxyanions: Interpretation of X-Ray Emission, ESCA, and NQR Spectra and of the Geochemistry of Beryllium and Boron

DAVID J. VAUGHAN, AND JOHN A. TOSSELL
Department of Earth and Planetary Sciences, Massachusetts Institute of Technology, Cambridge, Massachusetts 02139

Abstract

Quantitative molecular orbital (MO) calculations for the $[BeO_4]^{6-}$, $[BeO_3]^{4-}$, $[BO_4]^{5-}$ and $[BO_3]^{3-}$ ions are used to interpret the oxygen $K\alpha$ X-ray emission spectra of BeO and B_2O_3 and the core and valence level ESCA spectra of BeO. Good agreement between calculated and experimental data support both the spectral interpretations and the validity of the calculations. The nuclear quadrupole coupling constant for trigonally coordinated boron in the $[BO_3]^{-3}$ group has also been calculated and reasonable agreement was found with experiment. The application of these MO calculations to beryllium and boron geochemistry is discussed.

Introduction

The geochemistry of beryllium is dominated by the $[BeO_4]^{6-}$ ion. This ion occurs in the most important beryllium-containing minerals, beryl ($Al_2Be_3Si_6O_{18}$) and chrysoberyl (Al_2BeO_4), and in such simple beryllium compounds as BeO (the rare mineral "bromellite"). A trigonal BeO_3 group has been observed in some synthetic beryllium oxides (Harris and Yakel, 1966, 1967, 1969) but is extremely rare. The geochemistry of boron is also dominated by oxyanion groups but in this case both tetrahedral $[BO_4]^{5-}$ and plane triangular $[BO_3]^{3-}$ ions are common. For example, both three- and fourfold coordinated boron occurs in borax ($Na_2B_4O_7 \cdot 10H_2O$).

In this paper the chemical bonding of beryllium and oxygen in the $[BeO_4]^{6-}$ ion and the bonding of boron and oxygen in the $[BO_4]^{5-}$ and $[BO_3]^{3-}$ ions are examined using approximate, self-consistent, molecular orbital (MO) calculations. The calculation for a $[BeO_4]^{6-}$ tetrahedron is compared with the experimentally determined X-ray emission and ESCA spectra for BeO. Only scant X-ray emission data are available for boron (in B_2O_3) which are also compared with the calculations presented here. However, in the case of the $[BO_3]^{3-}$ ion, it has also been possible to compare the results of the calculation with NQR spectral data. In all the above cases, the reasonably good agreement between calculation and experiment validates the calculation and clarifies interpretation of the experimental data.

Molecular Orbital Calculations

The approximate MO calculation used in this study incorporates elements of the CNDO/2 method of Pople and Segal (1966) and the NEMO method of Newton *et al* (1966). In this method all the important electrostatic contributions to the energy are included. Thus, all electrons are included explicitly, full self-consistency of the charge distribution is required, and no empirical parameterization is introduced. Further details of the method have been presented by Tossell (1973b) and will not be discussed here. It has been successfully used to interpret the X-ray emission spectra of silicon, aluminum, and magnesium oxyanions (Tossell, 1973a, b).

A calculation was performed on the regular tetrahedral anion $[BeO_4]^{6-}$ and the eigenvalues and orbital compositions for this unit are given in Table 1. Because the method does not give absolute MO energies (ϵ_i) relative to the Fermi level, the energies are presented relative to one of the non-bonding orbitals taken as an arbitrary zero (*i.e.*, as $\Delta\epsilon_i$). By analogy with calculations for the SO_4^{2-} ion, incorrect ordering of the $5t_2$ and $1t_1$ orbitals is expected using the present method (Tossell, unpublished results; Gelius *et al*, 1971). For the tetrahedron $[BeO_4]^{6-}$, the valence orbitals may be considered as falling into the following groups: (1) $3a_1$ and $2t_2$, O2*s* orbitals; (2) $3t_2$ and $4a_1$, σ-bonding orbitals; (3) $1e$ and $1t_1$, non-bonding orbitals; (4) $4t_2$, weakly π-bonding orbital; (5) $5t_2$ and $5a_1$, σ-antibonding orbitals (empty).

TABLE 1. Relative Eigenvalues ($\Delta\epsilon_i$) and Orbital Compositions for $[BeO_4]^{6-}$ and $[BO_4]^{5-}$*

MO	$[BeO_4]^{-6}$ Calculations † $\Delta\epsilon_i$ (ev)**	% Orbital Comp. Be 2s	Be 2p	O 2s	O 2p	$[BO_4]^{-5}$ Calculations †† $\Delta\epsilon_i$ (ev)**	% Orbital Comp. B 2s	B 2p	O 2s	O 2p
$5a_1$	36.18	95	--	--	5	54.67	95	--	--	5
$5t_2$	31.28	--	86	--	14	43.24	--	85	--	15
$4t_2$	0.55	--	1	1	98	1.36	--	1	1	98
$1t_1$	0	--	--	--	100	0	--	--	--	100
$1e$	-1.63	--	--	--	100	-3.0	--	--	--	100
$4a_1$	-3.26	8	--	--	92	-5.99	9	--	2	89
$3t_2$	-4.35	--	17	--	83	-6.80	--	18	--	82
$2t_2$	-22.57	--	3	97	--	-23.40	--	2	98	--
$3a_1$	-24.21	3	--	97	--	-27.20	3	--	97	--
$2a_1$	-123.76		Bels			-211.62		Bls		
$1a_1+1t_2$	-535.29		Ols			-535.84		Ols		

* *MO's up to and including $4t_2$ are filled by electrons.*

† *Be-O internuclear distance is 1.65 Å.*

†† *B-O internuclear distance is 1.46 Å.*

** *The $1t_1$ eigenvalue is taken as the arbitrary zero of the energy scale in this table.*

TABLE 2. Relative Eigenvalues ($\Delta\epsilon_i$) and Orbital Compositions for $[BO_3]^{3-}$*

MO	$[BO_3]^{-3}$ Calculations † $\Delta\epsilon_i$ (ev)**	% Orbital Comp. B 2s	B 2p	O 2s	O 2p
$5e'$	51.68	--	87	--	13
$5a_1'$	45.16	92	--	--	8
$2a_2''$	22.04	--	65	--	35
$4e'$	1.09	--	2	1	97
$1a_2''$	0	--	--	--	100
$1e''$	-1.63	--	--	--	100
$4a_1'$	-5.16	12	--	--	88
$3e'$	-6.52	--	16	--	84
$1a_2'$	-9.24	--	35	--	65
$2e'$	-25.29	--	4	96	--
$3a_1'$	-27.74	--	3	97	--
$2a_1'$	-211.88		Bls		
$1a_1'+1e$	-538.56		Ols		

* *MO's up to and including 5e are filled by electrons.*

† *B-O internuclear distance is 1.36 Å.*

** *The $1a_2'$ eigenvalue is taken as the arbitrary zero of the energy scale.*

A similar calculation on a regular $[BO_4]^{5-}$ tetrahedron yielded the results in Table 2. It can be seen that the compositions of the molecular orbitals in terms of atomic orbitals are virtually identical and their order is the same as in $[BeO_4]^{6-}$. The valence orbitals may therefore be broken down into the same five groups as in $[BeO_4]^{6-}$. However, the relative energies of the molecular orbitals are very different in the two cases, a fact which will be discussed later.

Calculated moelcular orbitals for a regular triangular $[BO_3]^{3-}$ group are presented in Table 3. The valence orbitals may be grouped as follows: (1) $3a_1'$ and $2e'$, O2*s* orbitals; (2) $1a_2''$, $3e'$ and $4a_1'$, σ and π-bonding orbitals; (3) $1e''$ and $1a_2'$, non-bonding orbitals; (4) $4e'$, weakly σ-bonding orbital; (5) $2a_2''$, $5a_1'$ and $5e'$, σ and π-antibonding orbitals (empty).

TABLE 3. Experimental and Calculated Relative Energies (ev) and Intensities of O$K\alpha$ X-Ray Emission Spectra in BeO

Assignment	Calculated ΔE(e.v.)	Calculated I	Observed ΔE(e.v.)	Observed I
$4t_2 \rightarrow 1a_1+1t_2$	+0.55	98%	+0.5	100%
$1t_1 \rightarrow 1a_1+1t_2$	0	100%	0	
$1e \rightarrow 1a_1+1t_2$	-1.63	66%	(not resolvable)	
$4a_1 \rightarrow 1a_1+1t_2$	-3.26	31%	-3.0	20%
$3t_2 \rightarrow 1a_1+1t_2$	-4.35	83%	-4.7	

Comparison with X-Ray Emission and ESCA Spectra

The quantitative MO results of Table 1 may be used to assign transitions in the X-ray spectrum of oxygen in BeO. Mo theory has already been used to assign transitions in the oxygen spectra in silicates by Urch (1970), Dodd and Glen (1968), and Tossell (1973a). X-ray spectra are produced by transitions from a higher level to an inner shell vacancy and may be classified as *K*, *L*, or *M* depending upon the inner shell involved. The $K\alpha$ line arises from transitions of the type $2p \rightarrow 1s$ and the O$K\alpha$ energy is thus given by the eigenvalue difference of the group of MO's $4t_2$, $1t_1$, $1e$, $4a_1$, $3t_2$ and the $1a_1 + 1t_2$ MO. Due to the approximate nature of the calculation and to the neglect of the important relaxation effects associated with core ion states, agreement of the calculated absolute value of the transition energy with experiment is only approximate. For example, we calculate $E_{OK\alpha}$ in $[BeO_4]^{6-}$ to be 536-530 ev whereas experiment gives 530-520 ev (Koster, 1971). Comparison of the measured O$K\alpha$ spectrum in BeO due to Koster (1971) and that predicted by our calculations is good, as shown by Table 3 and Figure 1. In the ex-

TABLE 4. Relative Energies of MO's from ESCA Spectra of BeO Compared with Calculations

ESCA Binding Energy	Orbital	ΔE	Calculated ΔE (e.v.)
532.1	O1s($1a_1$+$1t_2$)	} 417.9	411.53
114.2	Be1s($2a_1$)	} 89.8	99.55
24.4	O2s($2t_2 3a_1$)		
11	$3t_2$, $4a_1$	} 3.4	3.45(average)
7.6	$1e$, $1t_1$, $4t_2$		

perimental spectrum, three major peaks (B, D, E in Fig. 1) were resolved. Peak B occurs at an almost constant position and intensity throughout a whole series of the O$K\alpha$ spectra (BeO, Li_2CO_3, CaO, SrO, BaO, BaO_2, MnO, *etc*) measured by Koster (1971). The height of peak B depends also upon the analyzing crystal. Liefeld *et al* (1970) attributed this peak to a reflectivity spike and Holliday (1967), who also studied the O$K\alpha$ spectrum from BeO, did not observe this peak when using a grating rather than a KAP crystal. These observations, together with our calculations, show that peak B of Koster is not a true feature of the spectrum but a function of the analyzing crystal used.

The peak D observed by Koster may be attributed principally to $4t_2$ and $1t_1 \rightarrow 1a_1 + 1t_2$ transitions and peak E, to the $3t_2 \rightarrow 1a_1 + 1t_2$ transition. The $1e$ and $4a_1 \rightarrow 1a_1 + 1t_2$ transitions can be considered to give rise to much of the intensity between D and E but cannot be separately resolved with present instrumentation.

The Be$K\beta$ spectrum in BeO has been determined by Lukirskii and Brytov (1964). Two peaks are observed with the lower energy $K\beta'$ peak separated from the main $K\beta$ peak by ~15 ev. We assign these two peaks to the $3t_2 \rightarrow$ Be $1s$ and $2t_2 \rightarrow$ Be $1s$ transitions and calculate their separation to be 18.2 ev. The relative Be $2p$ percent characters of these orbitals are also consistent with the relative intensity of the $K\beta$ and $K\beta'$ peaks observed by Lukirskii and Brytov (1964).

The valence band and core levels of BeO have also been studied by ESCA (Hamrin *et al*, 1970). In the ESCA experiment (also referred to as "X-ray photoelectron spectroscopy") the incident radiation causes electrons to be ejected. The ejected electrons have discrete kinetic energies which are measured in the experiment by an electron energy analyzer which scans the kinetic energy spectrum and records the peaks corresponding to electron energies (the "ESCA binding energies"). The technique is discussed in several review articles (Hollander and Jolly, 1970; Nordling, 1972). Mo calculations of the type employed in the present study were used by Tossell (1973a) to interpret shifts in the O1s ESCA spectra of silicates. The ESCA core binding energies are given in Table 4, where their separations are compared with values from the calculations. The valence orbital spectrum again has two main peaks which may be assigned to the $3t_2$ and $4a_1$ molecular orbitals (σ-bonding) and the $1e$, $1t_1$ and $4t_2$ molecular orbitals (mainly non-bonding). The experimentally determined separation between these peaks is in excellent agreement with the mean separation between the two MO groups given by calculation. This supports the assignments suggested to explain the BeO valence band spectrum and also establishes the validity of the MO calculation.

Unfortunately, the only X-ray emission or ESCA spectral data available for boron compounds is an O$K\alpha$ spectrum of B_2O_3 (Fischer, 1965). This was one of a large series of oxides examined in a preliminary study and was not discussed in detail. Crystalline B_2O_3, which contains BO_4 tetrahedral units, not glassy B_2O_3, which contains BO_3 trigonal units (Cotton and Wilkinson, 1962), was used (Dr. D. W. Fischer, personal communication). Figure 2 shows the comparison between the experimental spectrum

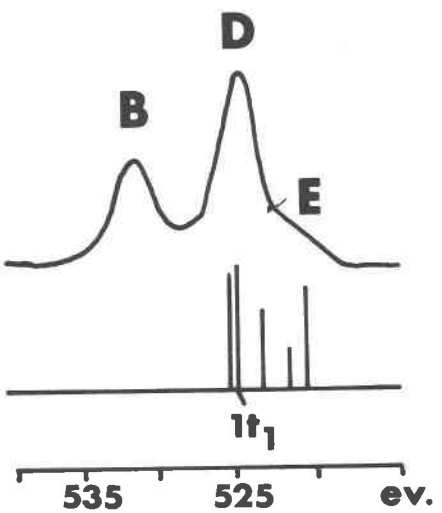

FIG. 1. The oxygen $K\alpha$ spectrum of BeO (after Koster, 1971). Beneath the spectrum are shown the positions and intensities of the X-ray emission peaks predicted by the MO calculations.

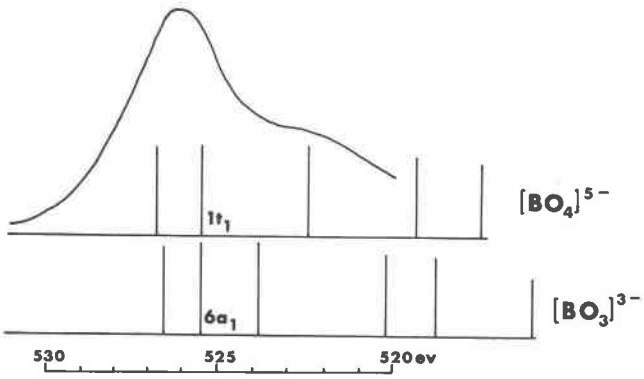

FIG. 2. The oxygen $K\alpha$ spectrum of B_2O_3 (after Fischer, 1965). Beneath the spectrum are shown the positions and intensities of the X-ray emission peaks predicted for both $[BO_4]^{5-}$ and $[BO_3]^{3-}$ by the MO calculations.

and the transitions predicted from the calculations for $[BO_4]^{5-}$ in crystalline B_2O_3 and for $[BO_3]^{3-}$ in glassy B_2O_3. It is clear from the figure that crystalline B_2O_3 was used in the experiment and that the two coordinations may be distinguished by X-ray emission spectroscopy when present separately. Agreement between experiment and calculation is therefore good, although the calculation predicts further peaks to the low velocity side of the spectrum, a region not studied by Fischer.

Comparison with NQR Spectra

For beryllium and boron compounds, nuclear quadrupole resonance (NQR) and nuclear magnetic resonance (NMR) yield nuclear quadrupole coupling constants which measure the strength of interaction between the electric quadrupole moment of the nucleus and the gradient of the electric field at the nuclear position. The electric field gradient (EFG) is a measure of the deviation of the charge density from cubic symmetry.

The ^{11}B quadrupole coupling constants represent the second largest body of magnetic resonance data in mineralogy, ^{27}Al being the most numerous. The values of the coupling constant C for ^{11}B are split into two groups: (1) C = 2.5 − 2.6 mc/sec for trigonally coordinated boron; (2) C = 0.50 − 0.70 mc/sec for boron in (distorted) tetrahedral coordination. The spread within each group is small. Using the formula developed some years ago by Townes and Dailey (1949), one can relate the electric field gradient at the ^{11}B nucleus to the anisotropy in B2p orbital populations given by the $[BO_3]^{3-}$ calculation. Using the measured atomic value of C for the free boron atom with one unbalanced 2p electron (C = 5.39 mc/sec), the predicted imbalance of σ and π B2p orbital populations for trigonally coordinated boron (average coupling constant = 2.55 mc/sec) is 0.47 electrons. The calculation on $[BO_3]^{3-}$ gave a p orbital imbalance of 0.43 electrons, in good agreement with the prediction of the Townes and Dailey model. The Be2p orbital perpendicular to the trigonal plane (π) has a population of 0.69 electrons, while those orbitals lying in the plane (σ) each contain 0.26 electrons. This indicates that the sign of the coupling constant is negative, but this conclusion awaits experimental verification.

Similar arguments suggest that the ^{9}Be quadrupole coupling constant will be much higher for trigonally coordinated than for tetrahedrally coordinated Be. NQR is therefore a possible technique for distinguishing the rare occurrences of trigonal BeO_3.

MO Theory and the Geochemistry of Beryllium and Boron

The geochemistry of beryllium has been discussed in detail by Beus (1960). Although more than forty beryllium minerals are known, all but two of them (beryl and chrysoberyl) are extremely rare. The rarity of beryllium is undoubtedly related to the lack of stability of the nuclei of all its isotopes, *i.e.*, it is related to the instability of beryllium in stellar depths and not its subsequent dissemination.

In natural compounds, beryllium is usually surrounded tetrahedrally by oxygen to form compact $[BeO_4]^{6-}$ tetrahedra. There are many similarities between the $[BeO_4]^{6-}$ and $[SiO_4]^{4-}$ tetrahedra, but also distinct differences. Similarities also exist between BeO_4 and AlO_4 tetrahedra, but the size discrepancy is greater in this case. Beryllium can therefore replace silicon to form beryllosilicates, but tetrahedra involving beryllium bonding to OH or F may also occur. Beryllium is found in isomorphous substitution in various silicate minerals (feldspars, garnets, pyroxenes, amphiboles, micas) but only rarely does the beryllium concentration exceed 0.1 percent.

Information on the relative "covalency" of the Be–O bond may be obtained from the calculations. Figure 3 is an attempt to compare the relative energies and separations of the molecular orbitals of the BeO_4^{6-} group with MgO_4^{6-}, AlO_4^{5-} and SiO_4^{4-}. The latter are taken from Tossell (1973b) who discusses the increasing covalency along the series Mg to Si. Following the same convention as Tossell, in Figure 3 the essentially nonbonding $1t_1$ orbital has been

taken as the arbitrary zero point of the energy scale. Although the series of Mg, Al, Si tetrahedral oxyanions involve bonding between oxygen 2*s* and 2*p* orbitals and metal 3*s* and 3*p* orbitals, whereas in BeO_4^{6-} the oxygen 2*s* and 2*p* orbitals form MO's with beryllium 2*s* and 2*p* orbitals, comparisons may still be drawn. The relative energies of the bonding, nonbonding and antibonding molecular orbitals in BeO_4^{6-} closely resemble those of AlO_4^{5-}. It is therefore more covalent than the Mg^{2+}–O^{2-} bond, but less covalent than the Si^{4+}–O^{2-} bond. Obviously, Be^{2+} is a much smaller cation than Al^{3+}, but the similarities in their molecular orbital structure are reflected in the formation of stable polyanionic groups containing OH^- ions. Gibbsite, diaspore, and boehmite are aluminum hydroxides. Beryllium forms such minerals as epididymite, $Na[BeSi_3O_7(OH)]$, which contains $BeO_2(OH)_2$ tetrahedra, and euclase, $AlBe(OH)[SiO_4]$, which contains $BeO_3(OH)$ groups. There are many other examples of Be^{2+}–OH^- bonds but Si^{4+}–OH^- bonding and substitution of OH for oxygen in SiO_4^{4-} tetrahedra are much less frequent.

The degree of covalence of the Be–O bonds in BeO_4^{6-} can also be seen in Table 1. The $3t_2$ and $4a_1$ bonding MO's are the result of appreciable mixing of O2*p* and Be2*s* and 2*p* atomic orbitals, as are the corresponding $5t_2$ and $5a_1$ antibonding MO's. The bonding of beryllium to oxygen takes place through sp^3 hybrids, a bonding scheme which together with the small size of the beryllium atom accounts for its occurrence almost solely in tetrahedral coordination in minerals. The Be–O covalency primarily affects the energies of the $3t_2$ and $4a_1$ bonding MO's, while the oxygen-oxygen interactions associated with "radius ratio" effects determine the energies of the higher lying nonbonding MO's.

A concise discussion of boron geochemistry is given by Christ and Harder (1969) and of the structural chemistry of the borates by Ross and Edwards (1967). Boron is also one of the less abundant elements, having a similar cosmic abundance to beryllium and for similar reasons. However, large quantities of boron are concentrated in deposits of hydrated borate minerals, particularly borax and kernite ($Na_2B_4O_7 \cdot 4H_2O$). Except for the rare minerals ferrucite and avogadrite, both of which contain $[BF_4]^{1-}$ tetrahedra, boron always occurs in chemical combination with oxygen, *i.e.* as a borate. Thus, as in the case of beryllium, parallels may be drawn with the silicates (and of course with beryllium minerals). Boron also forms a series of borosilicates, and like

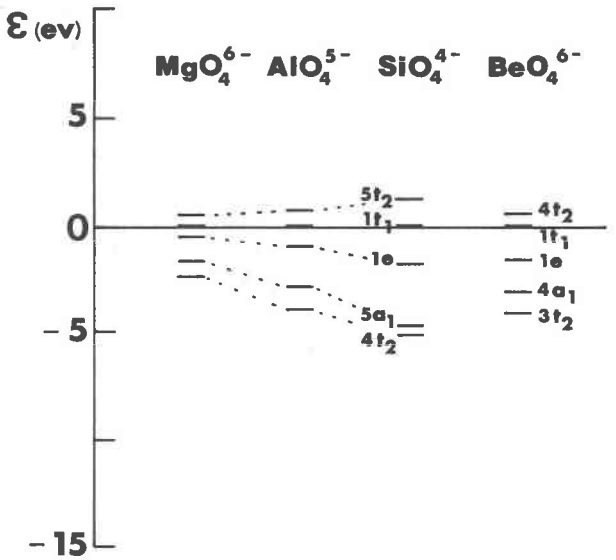

FIG. 3. Relative molecular orbital energies for the $[MgO_4]^{6-}$, $[AlO_4]^{5-}$, $[SiO_4]^{4-}$ and $[BeO_4]^{6-}$ ions. The $1t_1$ MO is taken as an arbitrary zero point.

beryllium, but unlike silicon, it frequently forms tetrahedral groups containing OH^- ions. Comparison of the MO data for $[BeO_4]^{6-}$ and $[BO_4]^{5-}$ tetrahedra shows that the oxyanions have virtually identical MO structures in terms of their atomic orbital compositions. However, the relative energies and separations

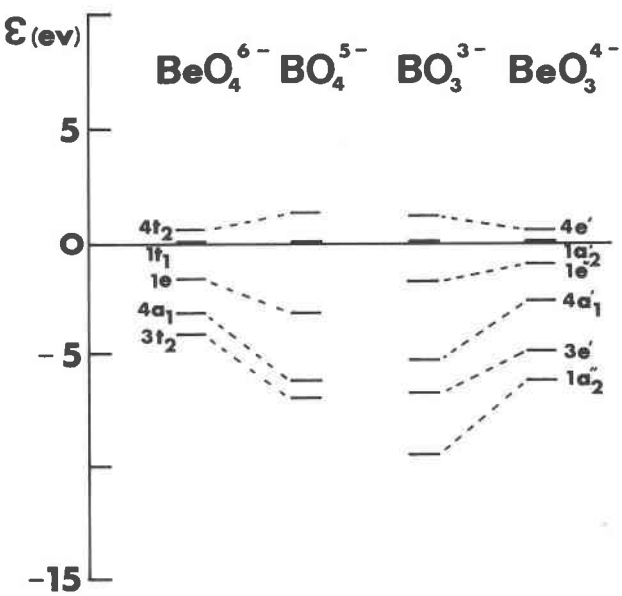

FIG. 4. Relative molecular orbital energies for the $[BeO_4]^{6-}$, $[BO_4]^{5-}$, $[BeO_3]^{4-}$ and $[BO_3]^{3-}$ ions. The $1t_1$ MO and the $6a_1$ MO are taken as the arbitrary zero points.

of the MO's are extremely different (Fig. 4). The $[BO_4]^{5-}$ ion appears to be even more covalent than $[SiO_4]^{4-}$.

The major difference between the crystal chemistry of boron and that of beryllium and silicon is the common occurrence of the trigonal $[BO_3]^{3-}$ ion. The MO structure of the $[BO_3]^{3-}$ ion is very different from the $[BO_4]^{5-}$ ion and the other tetrahedral oxyanions. Table 2 shows that the σ-bonding and σ-antibonding orbitals exhibit a greater degree of mixing between O2p and B2s and 2p atomic orbitals. The relative MO energy separation shown in Figure 4 is very different from any of the tetrahedral groups (taking the non-bonding $6a_1$ orbital as the zero point of the energy scale). This is the most covalent of all the oxyanions shown and the large degree of stabilization gained by the $5a_1$, $3e$, and $4a_1$ σ-bonding orbitals is apparently more than enough to compensate for the fact that there are now only three B–O bonds. The relative MO energies in a $[BeO_3]^{4-}$ group are also shown in Figure 4 and in this case the stabilization of the σ-bonding orbitals is somewhat less, perhaps accounting for the rarity of this coordination in beryllium minerals.

Molecular orbital theory therefore provides models of the chemical bonding of beryllium and boron in minerals which include the effects associated with radius ratio rules and covalency. The models are in good agreement with experimental data from spectral studies and with the observed geochemical properties of these elements.

Acknowledgments

The research was supported by NASA grant NGL22-009-187. Professor Roger G. Burns provided valuable comments on the manuscript.

References

BEUS, A. A. (1960) *Geochemistry of Beryllium and Genetic Types of Beryllium Deposits.* U.S.S.R. Acad. Sci. 1966 translation edited by L. R. Page, W. H. Freeman and Co., San Francisco.

CHRIST, C. L., AND H. HARDER (1969) Boron, *In, Handbook of Geochemistry, II-I,* Ed. K. H. Wedepohl, Springer-Verlag, Berlin.

COTTON, F. A., AND G. WILKINSON (1962) *Advanced Inorganic Chemistry.* Interscience, New York.

DODD, C. G., AND G. L. GLENN (1968) Chemical bonding studies of silicates and oxides by X-ray K-emission spectroscopy. *J. Appl. Phys.* **39,** 5377–5384.

FISCHER, D. W. (1965) Effect of chemical combination on the X-ray emission spectra of oxygen and fluorine. *J. Chem. Phys.* **42,** 3814–3821.

GELIUS, U., B. ROOS, AND P. SIEGBAHN (1971) MO-SCF-LCAO studies of sulfur compounds. *Theor. Chim. Acta,* **23,** 59–66.

HAMRIN, K., G. JOHANSSON, U. GELIUS, C. NORDLING, AND K. SIEGBAHN (1970) Valence bands and core levels of the isoelectronic series, LiF, BeO, BN, and graphite studied by ESCA. *Phys. Scripta,* **1,** 227–280.

HARRIS, L. A., AND H. L. YAKEL (1966) The crystal structure of calcium beryllate $Ca_{12}Be_{17}O_{29}$. *Acta Crystallogr.* **20,** 296–301.

———, AND ——— (1967) The crystal structure of Y_2BeO_4. *Acta Crystallogr.* **22,** 354–360.

———, AND ——— (1969) The crystal structure of $SrBe_3O_4$. *Acta Crystallogr.* **B25,** 1647–1651.

HOLLANDER, J. M., AND W. L. JOLLY (1970) X-ray photoelectron spectroscopy. *Account. Chem Res.* **3,** 193–200.

HOLLIDAY, J. E. (1967) The use of soft X-ray fine structure in bonding determination and light element analysis. *Norelco Rep.* **14,** 84–91.

KOSTER, A. S. (1971) Influence of the chemical bond on the K emission spectrum of oxygen and fluorine. *J. Phys. Chem. Solids,* **32,** 2685–2692.

LIEFELD, R. J., S. HANZELY, T. B. KIRBY, AND D. MOTT (1970) X-ray spectrometric properties of potassium acid pthalate crystals. *Advan. X-ray Anal.* **13,** 373–381.

LUKIRSKII, A. P., AND I. A. BRYTOV (1964) Investigation of the energy structure of Be and BeO by ultra long wave X-ray spectroscopy. *Fiz. Tverd. Tela (U.S.S.R.),* **6,** 43–50.

NEWTON, M. D., F. P. BOER, AND W. N. LIPSCOMBE (1966) Molecular orbital theory for large molecules, approximation of the SCF LCAO Hamiltonian matrix. *J. Amer. Chem. Soc.* **88,** 2353–2360.

NORDLING, C. (1972) ESCA: Electron spectroscopy for chemical analysis. *Angew. Chem. Int. Ed.* **11,** 83–92.

POPLE, J. A., AND G. A. SEGAL (1966) Approximate self-consistent molecular orbital theory. III CNDO results for AB_2 and AB_3 Systems. *J. Chem. Phys.* **44,** 3289–3296.

ROSS, V. F., AND J. O. EDWARDS (1967) The structural chemistry of the borates, *In, The Chemistry of Boron and its Compounds,* Ed. E. L. Muetterties, John Wiley, New York.

TOSSELL, J. A. (1973a) Molecular orbital interpretation of X-ray emission and ESCA spectral shifts in silicates. *J. Phys. Chem. Solids,* **34,** 307–319.

——— (1973b) Interpretation of K X-ray emission spectra and chemical bonding in oxides of Mg, Al and Si using quantitative molecular orbital theory. *Geochim. Cosmochim. Acta,* **37,** 583–594.

TOWNES, C. H., AND B. P. DAILEY (1949) Determination of electronic structure of molecules from nuclear quadrupole effects. *J. Chem. Phys.* **17,** 782–796.

URCH, D. S. (1970) The origin and intensities of low energy satellite lines in X-ray emission spectra: a molecular orbital interpretation. *J. Phys. C.,* **3,** 1275–1291.

Manuscript received, January 8, 1973;
accepted for publication, March 14, 1973.